Threshold and Trend Artifacts in Localized Multi-Frequency Bioimpedance Measurements ⋆

Todd J. Freeborn * **Shelby Critcher** *

* *Department of Electrical and Computer Engineering, University of Alabama, Tuscaloosa, AL 35404 USA (e-mail: tjfreeborn1@eng.ua.edu).*

Abstract: Localized tissue bioimpedance is being widely investigated as a technique to identify physiological features in support of health focused applications. In support of this method being translated into wearable systems for continuous monitoring, it is critical to not only collect measurements but also evaluate their quality. This is necessary to reduce errors in equipment or measurement conditions from contributing data artifacts to datasets that will be analyzed. Two methods for artifact identification in resistance measurements of bioimpedance datasets are presented. These methods, based on thresholding and trend detection, are applied to localized knee bioimpedance datasets collected from two knee sites over 7 consecutive days in free-living conditions. Threshold artifacts were identified in 0.04% (longitudinal and transverse) and 0.69% (longitudinal) /3.50% (transverse) of the total data collected.

1. INTRODUCTION

The passive electrical impedance of biological tissues, often referred to as tissue bioimpedance, is being widely investigated as a technique to identify physiological features in support of health focused applications. A detailed review of these health applications are available in the recent review by Naranjo-Hernandez et al. (2019). Tissue bioimpedance, regardless of the site from which it was collected or the target application, are related to tissue fluid, tissue type, and tissue geometry. As such, changes in each characteristic of these features is expected to alter the tissue impedance and potentially serve as an indicator of that underlying mechanism of change (e.g. fluid shift, tissue damage, tissue swelling). It is this potential that drives continued research focused on bioimpedance applications for patient monitoring and identification of physiological changes over time. Increasingly, this research has focused on transitioning instrumentation and systems to collect these measurements from portable to wearable options (see Mabrouk et al. (2020a); Wang et al. (2021); Usman et al. (2020); Dheman et al. (2021)). Because of the unobtrusiveness of wearable sensing systems and their ability to collect data over extended periods of time, these systems provide new opportunities for personalised precision medicine (see Jeong et al. (2019)).

Beyond collecting bioimpedance measurements, it is critical to also evaluate their quality. Assessing data quality ensures errors in equipment or measurement conditions are handled appropriately, otherwise data artifacts can be introduced during processing and interpretation. This is especially important for wearable systems in which data will be collected unsupervised and processed using automated algorithms to provide bio-feedback or evaluated via post-processing well after collection. Sources of error in wearable bioimpedance systems could include motion artifacts, electrode disconnect events, electrode aging, cabling damage/disconnects, and electronics/sensor damage. While these types of events can be captured during direct supervision in a clinical or lab environment (with new measurements collected after correction or elimination of the error source), this is not possible during free-living. Therefore, there is a need to identify, report, and correct or remove data artifacts in bioimpedance datasets collected using wearable systems. Previous research in support of this aim by Hersek et al. (2015) utilized accelerometers to identify time-points in which postures for measurements will be similar (e.g. during motionless standing). However, this approach does not evaluate the quality of measurements in this detected position. So while identifying positions of participants is critical to evaluate measurements collected at different time-points, it does not determine if a period of activity may have resulted in an electrode disconnect or other event that impacts the collected data. This further need provides the motivation for this research.

In this work, two methods for identifying data artifacts in bioimpedance datasets using thresholding (based on a review of existing localized measurements) and trend detection (based on expected tissue properties) are detailed. Next, these methods are applied to a set of bioimpedance data collected across 7 consecutive days from the knee of a study participant using a wearable sensing system to determine the rate at which these potential data artifacts occurred and how they could impact the interpretation of bioimpedance data.

⋆ This research was supported by the National Institute On Aging of the National Institutes of Health under Award Number R21AG056265.

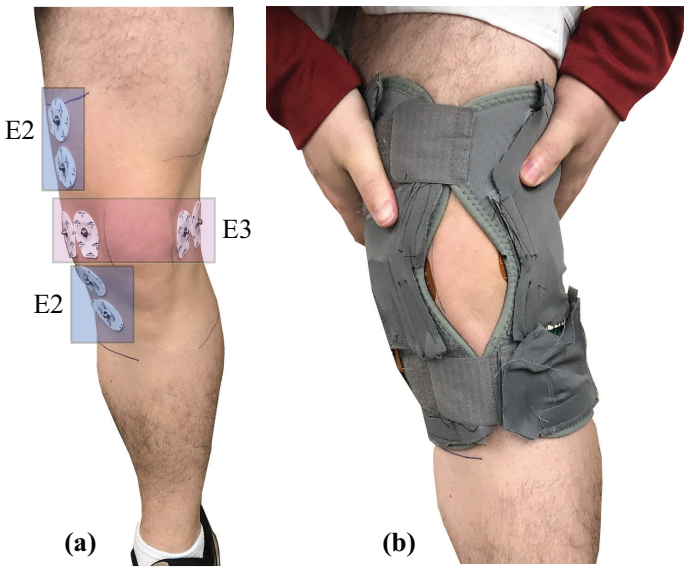

Fig. 1. a) Sample placement of E2 and E3 electrodes on knee sites and b) sample of knee brace (with electrodes integrated) for data collection during free-living.

2. FREE-LIVING DATA COLLECTION

To evaluate the rate of occurrence of potential data artifacts in free-living conditions using a wearable system, multi-frequency resistance measurements were collected from a single participant wearing an electronic sensing system integrated into a knee brace across 7 consecutive days. Prior to data collection, the study participant (Female, 24 years of age, 169 cm, 68.4 kg, 23.9 BMI) provided their written informed consent to be in the study. This participant reported no history of knee pain and no previous knee injuries. This research and its activities were approved by The University of Alabama's Institutional Review Board (UA IRB-18-013-ME).

2.1 Knee Measurement Platform

Resistance measurements were collected from two sites of the participants' knee using an electronic sensing system integrated into an off-the-shelf brace. A sample of this wearable sensing system is given in Fig. 1. In this system, two tetrapolar configurations of Ag/AgCl electrodes provided the interface to the tissue for an on-board MAX30001 integrated circuit to measure these sites. The MAX30001 is a single-chip integrated circuit (IC) with analog-front-end (AFE) circuitry designed for bioimpedance measurements. For further details regarding the MAX30001, readers are directed to works that have demonstrated and characterized the operation of the MAX30001 (see Critcher and Freeborn (2021)) and validated the use of analog-muxes to increase the number of tissue sites for monitoring (see Critcher and Freeborn (2020)). The system presented by Critcher and Freeborn (2020) is the platform utilized for data collection in this effort.

The specific locations of the two sets of tetrapolar electrodes are given in Fig. 1(a). The notation E2 and E3 refers to the electrode pairs along the longitudinal and transverse axes of the knee, respectively. The longitudinal pair were placed superior and inferior while the transverse pair were placed medially and laterally. During each of the 7 days of data collection, the participant affixed the system on their right knee after installing new electrodes each morning. After setup the participant resumed their typical daily activities (work, errands, travel, relaxation, etc.) for the day. While wearing the brace, multi-frequency resistance measurements from 1 kHz to 128 kHz were collected at approximately 3.5 minute intervals. A subset of those frequencies (8 kHz, 18 kHz, 40, kHz, 80 kHz, and 128 kHz) were analyzed in this work. The resistance data was saved to an on-board microSD card as an ascii-text file. At the end of each day, the participant would remove the brace, transfer the contents of the microSD card to a laptop computer, and upload the data to a secure cloud storage location established for the study.

The 7 days of processed and cleaned resistance data from both tissue sites using the E2 and E3 electrodes are detailed in Fig. 2. This represents 2026 measurement timepoints across these 7 days. Note though, that only 3 of the discrete frequencies (8 kHz, 40 kHz, and 128 kHz) are provided in Fig. 2. From the resistance datasets presented there are both intra-day and inter-day variability observed. For reference, the daily mean and standard deviation, at 8 kHz, of the E2 datasets ranges from $83.2 \pm 4.03\,\Omega$ (Day 5) to $101.5 \pm 3.68\,\Omega$ (Day1) with ranges from $56.5 \pm 4.31\,\Omega$ (Day5) to $79.2 \pm 4.09\,\Omega$ (Day 7) for the E3 datasets. This variance was expected, as the range of activities, activity intensities, and body positions throughout each day will impact the fluid distribution, tissue geometry, and tissue state (e.g. contracted or relaxed), which all impact the tissue resistance.

3. ARTIFACT IDENTIFICATION

3.1 Resistance Range Expectations Detection

Existing studies that have collected bioimpedance using tetrapolar configurations from human subjects have reported resistances of:

- Approximately 70 Ω to 100 Ω for 50 kHz resistances of lower and upper limb muscle groups of young and older adults reported by Kortman et al. (2013);
- Approximately 37 Ω to 68 Ω for 50 kHz resistances of lower limbs of injured and non-injured football players by Nescolarde et al. (2013);
- Approximately 27 Ω to 46 Ω in the range from 10 kHz to 100 kHz in studies of localized bicep tissues before and after fatiguing activity by Fu and Freeborn (2018);
- 45.87 ± 12.77 Ω and 46.26 ± 13.71 Ω for 50 kHz resistances of the right and left (transversal) thigh during test-retest studies by Honorato et al. (2021).

While this list is not exhaustive, the values of resistance across these studies are all within the range:

$$10\,\Omega < R_{1\text{kHz}-1\text{MHz}} < 150\,\Omega \tag{1}$$

Therefore, measured resistances (in the frequency band from 1 kHz to 100 kHz) that exceed this range (especially measurements > 1 kΩ) are likely to be data artifacts. The language localized is in reference to a small body

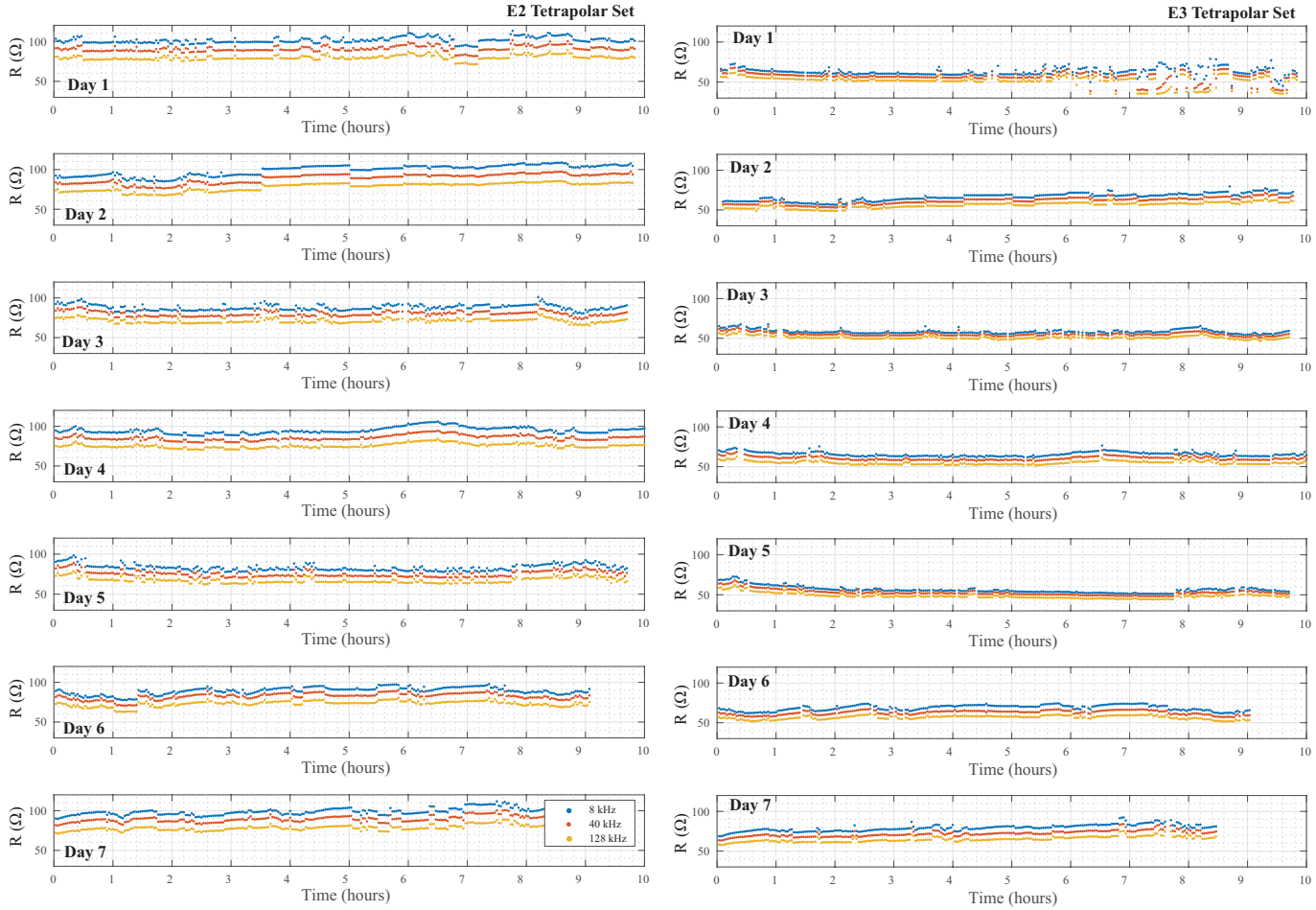

Fig. 2. 7-days of localized knee tissue resistance (8 kHz, 40 kHz, 128 kHz) collected at two sites from a single participant during free-living with artifacts removed.

segment being measured (e.g. region of the knee, region of the biceps, region of the lower limbs). Bioimpedance measurements can also be collected from larger segments (e.g. wrist to shoulder, ankle to thigh, hip to shoulder) and also the full-body (e.g. ankle to wrist). Both segmental and full-body bioimpedance measurements have larger resistance values than localized tissue measurements and will require different thresholds for evaluating data artifacts (and warrants future investigation). Additionally, the range given by (1) should not be utilized for measurements collected using bipolar configurations. Bipolar measurements also capture the tissue/electrode impedance which is typically larger than the tissue impedance and have reported impedance often above 1 kΩ.

A sample of a threshold artifact is detailed in Fig. 3, which presents the data from one multi-frequency sweep of the knee tissue of the study participant. In this figure, the resistance is presented on a logarithmic scale to highlight the range of values. Notice that the 40 kHz resistance exceeds 1 kΩ while each of the other 4 resistances are below 100 Ω. From a review of all of the participant data, a total of 9 resistance measurements exceeded the range given by (1). These 9 artifacts represent 0.04% of the total collected discrete resistances (the 2026 multi-frequency sweeps with 5 frequencies collected from 2 knee sites resulted in 20260 resistance measurements). While this type of artifact occurred in a very low amount of study data, it can still have a significant impact on data interpretation. As an example of the impact of these artifacts, consider the ratio h_α proposed by Mabrouk et al. (2020b) as a potential metric for differentiating healthy and injured ankles:

$$h_\alpha = \frac{\Delta R_{100\,\mathrm{kHz}}}{\Delta R_{5\,\mathrm{kHz}}} \tag{2}$$

where $\Delta R_{100\,\mathrm{kHz}}$ and $\Delta R_{5\,\mathrm{kHz}}$ are the range of resistances at 100 kHz and 5 kHz, respectively, measured across a fixed window of time. An artifact value in either frequency could cause a significant skewing of this metric and its interpretation. While the metric given by (2) was developed for applications to ankle injuries (and requires movement of the ankle through a range of positions for its generation), the knee resistance in this study can be used with the metric to highlight how data artifacts can impact it. It is important to note though, that this comparison is provided as a sample of the impact. Not that this metric can differentiate between healthy and injured knee tissues (which would warrant further research).

Consider the Day 1, E2 data given in Fig. 2 which has a $\Delta R_{128\,\mathrm{kHz}} = 18.54\ \Omega$ and $\Delta R_{8\,\mathrm{kHz}} = 19.78$. Using these values as close approximations of $\Delta R_{100\,\mathrm{kHz}}$ and $\Delta R_{5\,\mathrm{kHz}}$ in (2) yields $h_\alpha = 0.94$, but a low frequency

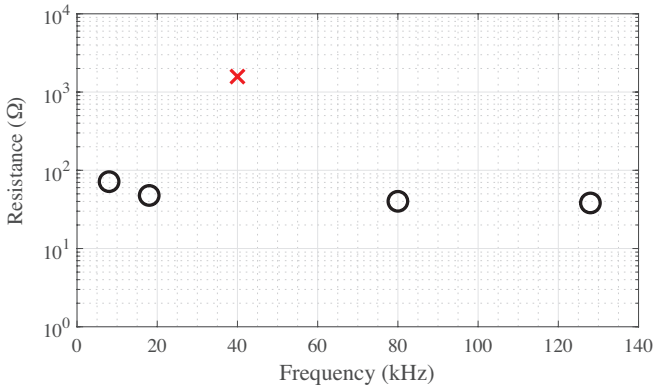

Fig. 3. Sample of range artifact in multi-frequency (8 kHz to 128 kHz) resistance of localized knee tissues, with the specific datapoint that is the artifact represented by the 'x' symbol.

threshold artifact with value of 1 kΩ would yield $h_\alpha = 0.02$. Consider that uninjured control subjects had a mean $h_\alpha = 0.955$ compared to a mean of $h_\alpha = 0.5$ for subjects with ankle injuries (see Mabrouk et al. (2020b)). So an artifact that significantly decreases this metric could result in classifying an ankle as injured if this artifact is not removed from the data for analysis. This highlights the need for identifying and removing this type of data artifact from a bioimpedance dataset.

3.2 Multi-Frequency Trend Detection

Tissue impedance is a frequency dependent quantity with decreasing resistance values reported for increasing frequency. This trend is also observed in the data reported in Fig. 2, specifically that $R_{8\,\mathrm{kHz}} > R_{40\,\mathrm{kHz}} > R_{128\,\mathrm{kHz}}$ across each of the days. This decreasing resistance trend can be utilized to also identify data artifacts in a single sweep of multi-frequency measurements, that is a finite number of measurements collected at different frequencies over a short-time interval. Because the time interval is short, it is assumed that the "state" of the tissue is constant. For a single sweep of N resistance measurements at increasing frequencies where $f_1 < f_2 < ... < f_N$, it is expected that:

$$R(f_1) > R(f_2) > ... > R(f_{N-1}) > R(f_N) \tag{3}$$

Based on this, values such that $R(f_{i+1}) > R(f_i)$, where $1 < i < N$, could indicate these measurements may have been contaminated. For example, the occurrence of a muscle contraction event. Muscle contraction has been shown to increase tissue resistance by Li et al. (2016) and Kitchin and Freeborn (2019). Depending on the length of contraction, this increase in resistance could have impacted one or more of the discrete frequency measurements. Alternatively, it could be a sign that the tissue may have come under compression by an external force during free living (e.g. bumping into an object).

Each of the 2026 frequency sweeps collected were reviewed to identify if the decreasing resistance detailed by (3) was satisfied. Those sweeps that did not satisfy this condition were noted as was the frequency of violation. Violations at the 18 kHz, 40 kHz, 80 kHz, and 128 kHz resistance are referred to as Type I, II, III, and IV artifacts, respectively. A total of 17 deviations were identified in the E2 data and 91 identified in the E3 data. These deviations in the multi-frequency trend impacted 14 and 71 total frequency sweeps (since multiple deviations can occur in a single sweep) which represents 0.69% and 3.50% of the total data over the 7-days. Samples of frequency sweeps with a Type I and Type II artifact are given in Fig. 4. The complete details of the number of each type of artifact are given in Table 1. It is interesting to note that measurements using the E3 electrodes had a larger number of this type of artifacts than the E2 electrodes. This might be an effect of the E3 electrodes location. During movement this location is expected to have the greatest alterations in terms of geometry of the tissue and the shifting of the brace/electrodes which could be the source of these artifacts.

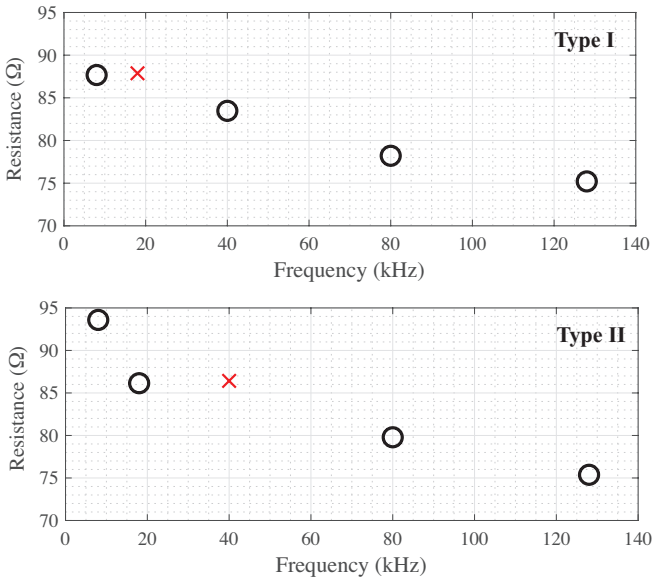

Fig. 4. Sample of Type 1 and Type 2 frequency artifacts in multi-frequency (8 kHz to 128 kHz) resistance of localized knee tissues, with the specific datapoint that is the artifact represented by the 'x' symbol.

Regardless of the source of this artifact, its presence in a multi-frequency sweep can impact the analysis and interpretation of the tissue bioimpedance. As an example, consider the equivalent circuit fitting utilized by Fu and Freeborn (2020) as a potential metric for identifying fatigue-related changes in skeletal muscle. Using this approach, optimization solvers are applied to determine the set of circuit parameters that provide the best fit of the Cole-impedance model (a three component equivalent circuit model, but see Freeborn (2013) for further details) to the experimental data. These circuit parameters are then utilized to compare tissue properties at different timepoints. Fu and Freeborn (2020) presented preliminary evidence that the constant phase element of this model may be sensitive to the cellular membrane changes that occur as a result of eccentric exercise. Data artifacts such as those shown in Fig. 4 will impact the outcome of the optimization solvers for this type of analysis and need to be removed or corrected.

Table 1. Number of trend artifacts in E2 and E3 knee tissue resistance across 7-days of monitoring

Location	Type I	Type II	Type III	Type IV
E2	10	2	1	4
E3	26	27	13	25

4. LIMITATIONS AND FUTURE WORK

An important limitation to note is that only data from a single participant has been analyzed and presented in this work. Further, this dataset appears to be a near ideal case of data collection in free-living conditions. That is, there are no periods of time with significant numbers of data artifacts which supports that no electrode disconnect or damage events and the brace was appropriately worn by the user across all days. This may not be the case for further data collection from different users using this wearable system. Therefore, further data collection from additional users is required to identify if threshold and trend artifacts occur at similar rates or if other types of artifacts are observed. As a sample of data that requires further investigation, consider the Day 1 data for the E3 tetrapolar electrode location between hours 7 and 10. While this data meets neither the threshold nor multi-frequency trend requirements to be classified as data artifacts, the difference between resistance measurements during this time period has a greater variability than all the other inter-day data. This could be another indicator of data artifacts that require further investigation.

While this work presented methods to identify data artifacts in localized bioimpedance measurements, it has not validated the cause of these artifacts which also warrants further study. Identifying the potential sources of error is necessary in improving the design of wearable systems and to inform potential approaches for bio-feedback to enhance the usability and effectiveness of these wearable systems. For example, reporting an electrode damage event so that the system can be corrected to improve the overall quality of data collection and decision making.

5. CONCLUSION

Data artifacts in the resistance component of tissue bioimpedance can significantly alter the interpretation of these measurements and require identification and correction/removal to limit this impact. Two types of data artifacts include values that exceed the threshold of expected resistance values and do not follow the multi-frequency trend of decreasing resistance. Reviewing data from 7-days of bioimpedance data from two sites of knee tissues of a single study participant, threshold and trend artifacts were identified in 0.04% (both knee sites) and 0.69% (E2)/3.50% (E3), respectively, of the data. Future work is required to determine if these artifact rates are consistent for the wearable design in this study and the root cause of these artifacts to inform future designs.

ACKNOWLEDGEMENTS

This research was supported by the National Institute On Aging of the National Institutes of Health under Award Number R21AG056265. The content is solely the responsibility of the authors and does not necessarily represent the official views of the National Institutes of Health.

REFERENCES

Critcher, S. and Freeborn, T.J. (2020). Multi-site impedance measurement system based on max30001 integrated-circuit (mwscas). In *2020 IEEE Midwest Symp. Circuits Systems*, 381–386. doi:10.1109/MWSCAS48704.2020.9184451.

Critcher, S. and Freeborn, T. (2021). Localized bioimpedance measurements with the max3000x integrated circuit: Characterization and demonstration. *Sensors*, 21(9), 3013. doi:10.3390/s21093013.

Dheman, K., Mayer, P., Eggimann, M., Schuerle, S., and Magno, M. (2021). Impedisense:a long lasting wireless wearable bio-impedance sensor node. *Sustainable Computing: Informatics and Systems*, 30, 100556. doi: https://doi.org/10.1016/j.suscom.2021.100556.

Freeborn, T.J. (2013). A survey of fractional-order circuit models for biology and biomedicine. *IEEE Journal on emerging and selected topics in circuits and systems*, 3(3), 416–424.

Fu, B. and Freeborn, T. (2020). Cole-impedance parameters representing biceps tissue bioimpednace in healthy adults and their alterations following eccentric exercise. *J. Adv. Res.*, 25, 285–293.

Fu, B. and Freeborn, T.J. (2018). Biceps tissue bioimpedance changes from isotonic exercise-induced fatigue at different intensities. *Biomedical Physics & Engineering Express*, 4(2), 025037.

Hersek, S., Töreyin, H., and Inan, O.T. (2015). A robust system for longitudinal knee joint edema and blood flow assessment based on vector bioimpedance measurements. *IEEE Transactions on biomedical circuits and systems*, 10(3), 545–555.

Honorato, R.d.C., Ferraz, A.S.M., Kassiano, W., Carvalho, D.P., and Ceccatto, V.M. (2021). Test-retest reliability of electrical impedance myography in hamstrings of healthy young men. *J. Electromyography Kinesiology*, 56, 102511. doi:10.1016/j.jelekin.2020.102511.

Jeong, I., Bychkov, D., and Searson, P. (2019). Wearable devices for precision medicine and health state monitoring. *IEEE Trans. Biomed. Eng.*, 66, 1242–1258. doi: 10.1109/TBME.2018.2871638.

Kitchin, N.M. and Freeborn, T.J. (2019). Contraction artifacts on biceps tissue bioimpedance collected using stepped-sine excitations. In *2019 SoutheastCon*, 1–6. doi:10.1109/SoutheastCon42311.2019.9020411.

Kortman, H.G.J., Wilder, S.C., Geisbush, T., Narayanaswami, P., and B., R.S. (2013). Age- and gender-associated differences in electrical impedance values of skeletal muscle. *Physiol. Meas.*, 34, 1611–1622. doi:10.1088/0967-3334/34/12/1611.

Li, L., Shin, H., Li, X., Li, S., and Zhou, P. (2016). Localized electrical impedance myography of the biceps brachii muscle during different levels of isometric contraction and fatigue. *Sensors*, 16(4), 581. doi: 10.3390/s16040581.

Mabrouk, S., Whittingslow, D., and Inan, O. (2020a). Robust method for mid-activity tracking and evaluation of ankle health post-injury. *IEEE Trans. Biomed. Eng.* doi:10.1109/TBME.2020.3027477.

Mabrouk, S., Hersek, S., Jeong, H.K., Whittingslow, D., Ganti, V.G., Wolkoff, P., and Inan, O.T. (2020b). Robust longitudinal ankle edema assessment using wearable bioimpedance spectroscopy. *IEEE Transactions on Biomedical Engineering*, 67(4), 1019–1029.

Naranjo-Hernandez, D., Reina-Tosina, J., and Min, M. (2019). Fundamentals, recent advances, and future challenges in bioimpedance devices for healthcare applications. *J. Sensors*, Article ID 9210258, 42. doi: 10.1155/2019/9210258.

Nescolarde, L., Yanguas, J., Lukaski, H., Alomar, X., Rosell-Ferrer, J., and Rodas, G. (2013). Localized bioimpedance to assess muscle injury. *Physiological measurement*, 34(2), 237.

Usman, M., Leone, M., Gupta, A.K., and Xue, W. (2020). Fabrication and analysis of wearable bioimpedance analyzers on paper and plastic substrates. *IEEE Sensors Letters*, 4(3), 1–4. doi:10.1109/LSENS.2020.2977232.

Wang, T.W., Chen, W.X., Chu, H.W., and Lin, S.F. (2021). Single-channel bioimpedance measurement for wearable continuous blood pressure monitoring. *IEEE Transactions on Instrumentation and Measurement*, 70, 1–9. doi:10.1109/TIM.2020.3035578.